Using the Gauss-Bonnet Theorem

Bradley McCoy

May 26, 2025

Contents

1 Introduction

In this section, we provide reasons to learn about the Gauss-Bonnet theorem. We then consider a special case of the theorem for simple polygons and we use this special case to prove Pick's theorem.

1.1 A Great Theorem

The Gauss-Bonnet theorem relates the curvature, a local property, of a surface to the Euler characteristic, a global property. If we travel over a surface and compute the curvature at each point we are able to combine our computations to learn about the topology of the surface as a whole. Conversely, if we know the topology of a surface we are able to guarantee the existence of a point on the surface with positive curvature. The goal of this work is to demonstrate that both of the directions described above are useful.

In symbols, a version of the Gauss-Bonnet theorem can be expressed as

$$\int_M K dA = 2\pi\chi(M) \tag{1}$$

where M is a smooth surface in $\mathbb{R}^3$ without boundary, K is Gaussian curvature and $\chi(M)$ is the Euler characteristic of M.

The Gauss-Bonnet theorem is a hub between seemingly disparate ideas, see Figure 1.1.

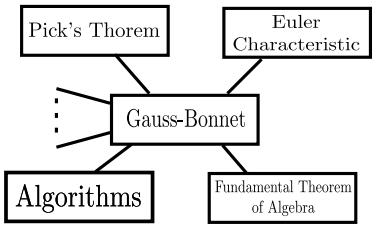

Figure 1.1: The Gauss-Bonnet theorem is a star.

What separates a great theorem form a mediocre theorem? In [36], Matoušek says that a theorem is a great theorem if there are

(1) several different equivalent versions,

(2) many different proofs,

(3) a host of extensions and generalizations, and

(4) numerous interesting applications.

By this criteria, the Gauss-Bonnet theorem is a great theorem. For (1), six different versions of the theorem are discussed in [48]. In addition to the version for smooth surfaces given in Equation 1, we highlight several discrete versions for triangulated surfaces.

As for (2), several fundamentally different proofs exist. One common approach is to first prove the theorem for simply connected domains with boundary, then triangulate a

surface and add up the contribution from each triangle. However, this proof seems to lack a geometric intuition that other proofs provide. [48], A second commonly seen proof is to use Stokes theorem [18, 42]. Many other proofs exist [29, 34, 28].

For (3), the theorem has been generalized in the following ways. The two notable examples are the Chern-Gauss-Bonnet theorem[15] and the Atiyah–Singer index theorem is an example [4]. A generalization to higher dimensions [29]. The discrete versions of the theorem discussed here can be thought of as extensions to more computationally friendly objects.

As for (4), applications, seven are given in [18]. For applications to physics see [46, 26]. This work provides examples related to the algorithms and combinatorics but we include others. I hope that the number of applications continues to grow, please share any that you feel ought to be included[1].

Thus, by Matoušek standard, the Gauss-Bonnet theorem is a great theorem. We highlight classic applications of the theorem as well as more recent applications that illustrate that topological methods in combinatorics is an active area of research.

Historically, Gauss proved the special case of a geodesic triangle[19, 25]. The version given in Equation 1 is due to Pierre Bonnet and Jacques Binet [8]. A case can be made that the theorem ought to be called the Bauss-Binet-Bonnet Theorem [48].

1.2 Simple Polygons

Some of us may remember the following special case of the Gauss-Bonnet theorem from middle school geometry. Consider a simple polygon P, an example is shown in Figure 1.2a.

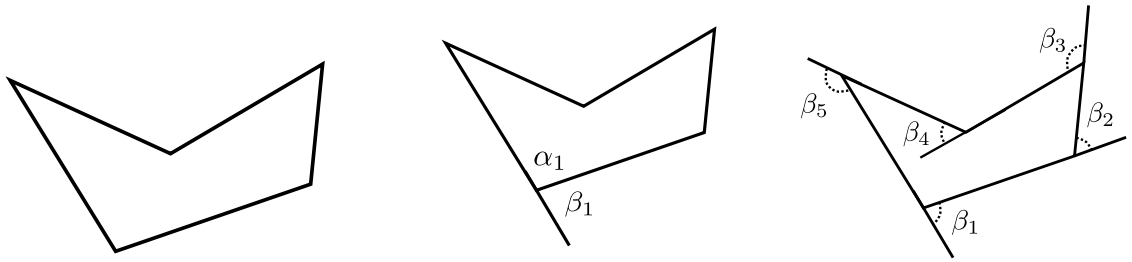

(a) A simple polygon. (b) Angles (c) Exterior angles.

Figure 1.2: (a) A simple polygon P. (b) The interior and exterior angles formed at a vertex. (c) The sum of the exterior angles of a simple polygon is 2π. Here $\beta_1+\beta_2+\beta_3+\beta_4+\beta_5 = 2\pi$ note that β_4 is negative.

If we extend one of the sides of P two complementary angles appear. The angle inside P is the *interior* angle and the complement is the *exterior angle*. An example is shown in Figure 1.2b. We differentiate between turning left and right. Vertices with interior angles greater than π are called *reflex*, see Figure 1.2c. At reflex vertices exterior angle is negative.

We now state a simple version of the Gauss-Bonnet theorem [27, 41],

[1]mccoy2ba@jmu.edu

Theorem 1.1 (Gauss-Bonnet for Polygons in the Plane)**.** *Let P be a simple polygon in the plane with n vertices, interior angles $\{\alpha_1, \alpha_2, \ldots, \alpha_n\}$ and exterior angles $\{\beta_1, \beta_2, \ldots, \beta_n\}$ then*

$$\sum_{i=1}^{n} \beta_i = 2\pi$$

and

$$\sum_{i=1}^{n} \alpha_i = \pi(n-2).$$

Proof. We traverse a polygon and rotate β_i at each vertex when we get back to where we started we will have preformed one complete revolution so $\sum_{i=1}^{n} \beta_i = 2\pi$. The exterior angles are complementary to the interior angles so for each i we have $\beta_i = \pi - \alpha_i$ and using the first part of the theorem, we have $\sum_{i=1}^{n}(\pi - \alpha_i) = n\pi - \sum_{i=1}^{n} \alpha_i = 2\pi$. Solving for $\sum_{i=1}^{n} \alpha_i$ gives the second part of the theorem.

□

No matter how we position the vertices of our polygon, if the boundary of the polygon stays closed and simple, the sum the exterior angles will be 2π. Even this simple version of the Gauss-Bonnet theorem has powerful consequences, as we now see in our first application, a proof of Pick's Theorem.

1.3 Pick's Theorem

Pick's Theorem gives a formula for the area of a polygon in the plane with vertices on the lattice $\mathbb{Z}^2$ [40]. We give a proof originally due to Blatter [7] and restated by Tabachnikov [44].

Theorem 1.2 (Pick's Theorem)**.** *Let P be a simple polygon in the plane with vertices on the lattice $\mathbb{Z}^2$, let I be the number of lattice points inside of P, let B be the number of lattice points on the boundary of P and let A denote the area of P. Then,*

$$A = I + \frac{B}{2} - 1.$$

See Figure 1.3 for an example.

Proof. Put a unit volume ice cube at each lattice point in the plane and let the ice melt. The water will evenly cover the plane with the amount of water inside the polygon equal to its area.

Consider a edge on the the polygon. The amount of water that flows into to polygon across this edge equals that amount of water that flows out of the polygon across this edge by symmetry. This is because the edge connects two lattice points, for each point the contributes flow across the edge in one direction there is a symmetric point that contributes and equal amount of flow in the opposite direction. So, the total flow across each edge is zero and the amount of water inside the polygon comes from interior cubes and the lattice vertices of the polygon.

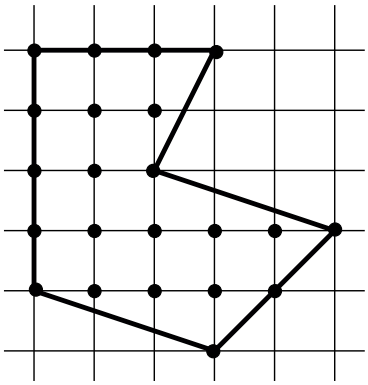

Figure 1.3: A polygon with vertices on the lattice. There are 10 interior vertices and 12 vertices on the boundary. By Pick's theorem the area of the polygon is $10 + \frac{12}{2} - 1 = 15$.

Each interior lattice point contributes one unit of water. Each lattice point on an edge, half of the water flows into the polygon and half flows outside of the polygon. Let α_i denote the interior angles at each vertex. Each vertex contributes $\frac{\alpha_i}{2\pi}$ units of water to the area. By the Gauss-Bonnet theorem, Theorem 1.1, the sum of the interior angles is $\pi(n-2)$. Thus, the vertex points contribute a total of

$$\frac{\pi(n-2)}{2\pi} = \frac{n}{2} - 1.$$

The theorem follows.

□

2 The Plane and the Sphere

The unit sphere and the plane are two popular surfaces. We often think of the sphere and the plane as subsets of $\mathbb{R}^3$, the sphere is the set

$$\mathbb{S}^2 = \{(x, y, z) \in \mathbb{R}^3 | x^2 + y^2 + z^2 = 1\}$$

and the xy-plane is

$$\mathbb{R}^2 = \{(x, y, z) \in \mathbb{R}^3 | z = 0\}.$$

Is it possible to continuously deform the sphere into the plane? The answer is no, as we will see. Stereographic projection is a map between almost all of the sphere and the plane. Given a point p on the sphere, we draw a straight line from the north pole $N = (0, 0, 1)$ through p, then find the intersection of this line with the plane. Every point on the sphere is mapped to a unique point in the plane except of the north pole. See Figure 2.2 for an illustration.

In order to gain intuition, we first consider the one dimensional version of stereographic projection between the unit circle $\mathbb{S}^1$ and and the real line. An example is shown in Figure 2.1. Consider a line from the north pole of the unit circle $(0, 1)$ that intersects the unit circle

at the point (u, v) parameterized by $p(t) = (1-t)(0,1) + t(u,v)$. By considering the y-coordinate we determine the t value were $p(t)$ intersects the x-axis, namely $t = \frac{1}{1-v}$. Then, the x-coordinate where $p(t)$ intersects the real line is

$$x = \frac{u}{1-v}.$$

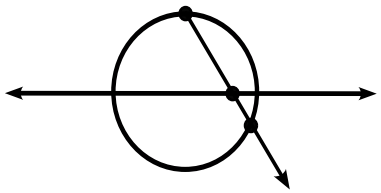

Figure 2.1: One dimensional stereographic projection.

A similar argument can be used to find the inverse map from the real line to the unit circle. Given an x-value on the real line we consider the parameterized line $p^{-1}(t) = (1-t)(0,1) + t(x,0)$ and compute the t value where p^{-1} is on the unit circle and $t \neq 0$. We find $t = \frac{2}{1+x^2}$ and the point (u, v) on the unit circle in terms of x is

$$u = \frac{2x}{1+x^2}, v = \frac{x^2-1}{1+x^2}.$$

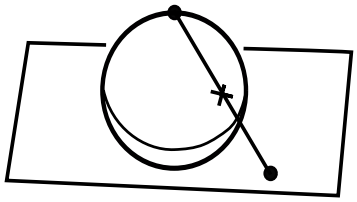

Figure 2.2: A point on the sphere is mapped to a point on the plane by stereographic projection.

We can use this idea to find formulas for stereographic projection from the unit sphere to the plane [16]. Consider the two sphere with the north pole $(0, 0, 1)$. The line from the north pole $(0, 0, 1)$ that intersects $(x, y, z) \in \mathbb{S}^2$ parametrized by $p(t) = (1-t)(0,0,1)+t(x,y,z)$. By considering the z coordinate we determine the t value where this line intersects $\mathbb{R}^2$, namely $t = \frac{1}{1-z}$. This gives the desired map and in equation form we have

$$p(x, y, z) \to \left(\frac{x}{1-z}, \frac{y}{1-z} \right).$$

Many of us have more experience doing computations on $\mathbb{R}$ and $\mathbb{R}^2$ as opposed to other objects. Stereographic projection enables us to transform many problems on the circle and the sphere into problems in $\mathbb{R}$ and $\mathbb{R}^2$ respectively. For example, suppose we wish to compute the integral of a constant function $c(x, y) = 1$ over the unit circle.

3 Cast of Characters

In the plane, if one scales a polygon, the area of the polygon changes but the angles of the polygon do not. On the unit sphere, we can relate the area of a simple polygon to the angles. This is because the sphere is curved. A triangle on the sphere is shown in Figure 3.1a.

(a) Spherical triangle. (b) A lune.

Figure 3.1: (a) A triangle on the sphere. (b) A lune with angle α.

A spherical *lune* is the region on a sphere bounded by two half great circles with angle α. The area of a lune is denoted $A(\alpha)$, see Figure 3.1b. On the unit sphere, the area of a lune is proportional to α. If $\alpha = 0$ the area is zero and if $\alpha = \pi$ the area is 4π. We can add the area of two lunes in terms of their angles, $A(\alpha_1 + \alpha_2) = A(\alpha_1) + A(\alpha_2)$ so A is linear and $A(\alpha) = 4\alpha$.

The following relates the area of a triangle on the sphere to the angles.

Lemma 3.1 (Area of Spherical Triangle)**.** *On the unit sphere, the area of a triangle with interior angles $\alpha_1, \alpha_2, \alpha_3$ is $A = \alpha_1 + \alpha_2 + \alpha_3 - \pi$.*

Proof. Any two edges of the the triangle form a lune. The collection of all three lunes covers the entire sphere with triangle and the antipodal triangle covered three times. The surface area of the unit sphere is 4π. Thus, $4\pi = 4\alpha_1 + 4\alpha_2 + 4\alpha_3 - 4A$ and $A = \alpha_1 + \alpha_2 + \alpha_3 - \pi$. □

As in the plane, any polygon on the sphere with n vertices can be decomposed into $n-2$ triangles [39]. This gives a formula for the area of a simple polygon on the sphere with interior angles $\alpha_1, \alpha_2, \ldots, \alpha_n$.

$$A = (2-n)\pi + \sum_{i=1}^{n} \alpha_i. \tag{2}$$

This difference between the plane and the sphere illustrates the need to quantify how much a surface is curving. What do we require of a definition of curvature? A straight line should have zero curvature and large circles should have less curvature than smaller circles. We also need to differentiate between curving to the left and curving to the right.

For any point on a smooth one dimensional curve in the plane, we can approximate the curve with a circle. The best approximating circle is the *osculating circle*. A natural definition of the *curvature* is the inverse of the radius of the osculating circle $k = \frac{1}{r}$. See Figure 3.2 for an example. The osculating circle meets the requirements for a definition of curvature as long as we allow the straight line to have an osculating circle with infinite

radius. We determine the sign of the curvature by which side of the curve the osculating circle is on.

The above definition provides great intuition for the curvature of curves and surfaces. Computing this value depends on how a curve or surface is represented.

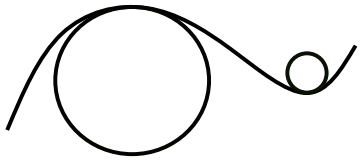

Figure 3.2: A curve with two osculating circles. The curvature at these points have opposite sign.

A curve in $\mathbb{R}^3$ is often presented as a function $\gamma(t) = (x(t), y(t), z(t))$. We say that a curve is *smooth* on an open interval I if γ' it is continuous and $\gamma'(t) \neq (0,0,0)$ on I. If γ is smooth it has a well-defined unit tangent vector $T(t) = \frac{\gamma'(t)}{|\gamma'(t)|}$. A second way to define the *curvature* at a point is as the signed magnitude of the rate of change of the unit tangent vector

$$\kappa = \pm |T'(t)|. \tag{3}$$

where t is arc length.

For example, take a circle of radius r, parameterized by

$$C(t) = (r\cos(t), r\sin(t), 0)\,.$$

We have

$$\frac{dC}{dt} = C'(t) = (-r\sin(t), r\cos(t), 0)$$

and $|C'(t)| = r$. Then $T(t) = (-\sin(t), \cos(t), 0)$ and $T'(t) = (-\cos(t), -\sin(t), 0)$. So, $\kappa(t) = \frac{1}{r}$ and, in this case, our definition of curvature agrees with the osculating circle intuition given above. Equation 3 can be rewritten in the following more computational friendly form

$$\kappa(t) = \frac{|\gamma'(t) \times \gamma''(t)|}{|\gamma'(t)|^3}. \tag{4}$$

We traverse γ at unit speed so that the length of the velocity vector is one, $\gamma'(t)^2 = 1$, and by the chain rule, $\gamma' \cdot \gamma'' = 0$. This implies γ' and γ'' are orthogonal. Thus, the vector $\gamma'' = N$ is normal to the γ. By taking the cross product of N and T we obtain a vector B called the binormal vector.

This osculating-circle idea can be extend to surfaces in $\mathbb{R}^3$, by considering the *osculating sphere*, But notice that at saddle points on a surface it is not clear which sphere best approximates the surface. See Figure 3.3 for two equally reasonable ways to approximate a saddle with a sphere.

(a) (b)

Figure 3.3: (a) The osculating sphere above the saddle. (b) The osculating sphere above the saddle.

3.1 Gaussian Curvature

One dimensional curves are represented by differentiable parameterized functions $\gamma : I \subset \mathbb{R} \to \mathbb{R}^3$, we would now like to parameterize a surface. Similarly, a *parameterized surface* S is a collection of maps such that for each point $p \in S$ we have a neighborhood $X \subset S$ and a map $r : U \subset \mathbb{R}^2 \to X \subset \mathbb{R}^3$, $r(u, v) = (x(u, v), y(u, v), z(u, v))$ where

- r is a homeomorphism
- r has derivatives of all orders
- every point in S is contained in the domain of at least one map.

The maps in the third item are called *charts*. If the differential $dr_q : \mathbb{R}^2 \to \mathbb{R}^3$ is one-to-one for all $q \in U$ then we say r is *regular*. In other words, let (u, v) be coordinates of $U \subset \mathbb{R}^2$, a surface is regular if $\frac{\partial r}{\partial u}$ and $\frac{\partial r}{\partial v}$ are linearly independent for all $p \in U$. Once we choose a chart we define a clockwise orientation to be positive. If the clockwise orientation can be consistently extended to the entire surface, we say the surface is *orientable*.

Example 3.2 (The Sphere)**.** The unit two sphere $\mathbb{S}^2 \subset \mathbb{R}^3$ is the set $\{(x, y, z) \in \mathbb{R}^3 | x^2 + y^2 + z^2 = 1\}$. We can define six charts to parameterize $\mathbb{S}^2$. For $u, v \in [-1, 1]$, we have

$$r_z(u, v) = (u, v, \sqrt{1 - u^2 - v^2}) \quad r_{-z}(u, v) = (u, v, -\sqrt{1 - u^2 - v^2}) \quad r_x(u, v) = (\sqrt{1 - u^2 - v^2}, u, v)$$

$$r_{-x}(u, v) = (-\sqrt{1 - u^2 - v^2}, u, v) \quad r_y(u, v) = (u, \sqrt{1 - u^2 - v^2}, v) \quad r_{-y}(u, v) = (u, -\sqrt{1 - u^2 - v^2}, v).$$

The chart r_z is shown in Figure 3.4

One can verify that these parameterizations fulfill the requirements for the sphere to be a regular surface.

A *tangent vector* to S at p is a map $\xi : (-\epsilon, \epsilon) \to S$ with $\xi(0) = p$. The set of all tangent vectors is the *tangent plane* and it corresponds to the image of the differential map $d\phi_q(\mathbb{R}^2) \subset \mathbb{R}^3$ (prop. 1 [18]). By choosing two linearly independent paths through $p \in S$ we obtain a basis for the tangent plane and define a normal vector N at p. Every plane containing the normal vector will intersect the surface. The intersection of the surface and each normal plane is a curve in $\mathbb{R}^3$ gives a one dimensional curve called the *normal section*, see Figure 3.5 for an example. Let κ_1 denote the maximum curvature of all normal sections

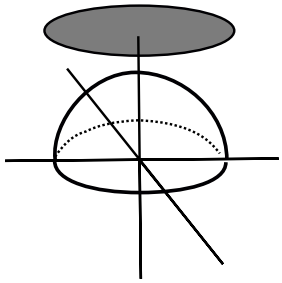

Figure 3.4: A chart of $\mathbb{S}^2$.

and let κ_2 denote the minimum. The *Gaussian curvature* of a point on a surface is $K = \kappa_1\kappa_2$. One can check that the Gaussian curvature of the plane is zero and that larger circles have less curvature than smaller ones.

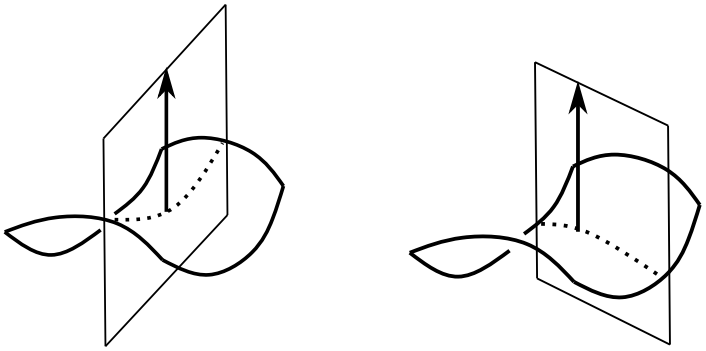

(a) (b)

Figure 3.5: (a) The osculating sphere above the saddle. (b) The osculating sphere above the saddle.

We now consider computing the Gaussian curvature. A *quadratic form* to be polynomial of degree two, of the form $p(u, v) = c_1u^2 + c_2uv + c_3v^2$ where $c_i \in R$. We define a quadratic form, the first fundamental form, using $r(u, v)$.

Let $r(u, v)$ be a parameterized surface. Let $E = r_u \cdot r_u, F = r_u \cdot r_v$ and $G = r_v \cdot r_v$. The *first fundamental form* is the quadratic form $\mathrm{I} = Edu^2 + 2Fdudv + Gdv^2$. We summarize the first fundamental form as a matrix

$$\mathrm{I} = \begin{bmatrix} E & F \\ F & G \end{bmatrix}.$$

The first fundamental form enables us to compute many interesting things about our surface including arc length, angles between curves, and area on a surface. For example, given a 'small' parallelogram M on S with corners $r(u, v), r(u + \epsilon u, v), r(u, v + \epsilon v)$ and $r(u + \epsilon u, v + \epsilon v)$ the rate of change of the area of M is

$$dA = \sqrt{EG - F^2}dudv.$$

In Example 3.4, we will use the first fundamental form to compute the arc length of some curves.

Gauss's Egregious (remarkable) Theorem states that the Gaussian curvature only depends of the first fundamental form. Thus, curvature can be computed entirely by measuring angles, distance and their derivatives without any reference to the way that the surface is embedded in $\mathbb{R}^3$. Because of this property we say that Gaussian curvature is an *intrinsic* property of a surface. The Brioschi formula gives the Gaussian curvature using only the first fundamental form

$$K = \frac{\begin{vmatrix} -\frac{1}{2}E_{vv} + F_{uv} - \frac{1}{2}G_{uu} & \frac{1}{2}E_u & F_u - \frac{1}{2}E_v \\ F_v - \frac{1}{2}G_u & E & F \\ \frac{1}{2}G_v & F & G \end{vmatrix} - \begin{vmatrix} 0 & \frac{1}{2}E_v & \frac{1}{2}G_u \\ \frac{1}{2}E_v & E & F \\ \frac{1}{2}G_u & F & G \end{vmatrix}}{(EG - F^2)^2} \tag{5}$$

While we can compute Gaussian curvature using only the first fundamental form, the second fundamental form is convenient for computations. To this end, the unit normal vector at p is given by

$$n(p) = \frac{r_u \times r_v}{|r_u \times r_v|}.$$

Let $L = r_{uu} \cdot n, M = r_{uv} \cdot n$ and $N = r_{vv} \cdot n$ the *second fundamental form* is $\mathrm{II} = Ldu^2 + 2Mdudv + Ndv^2$, in matrix form

$$\mathrm{II} = \begin{bmatrix} L & M \\ M & N \end{bmatrix}.$$

Combining the first and second fundamental forms we have the *Gaussian curvature* of a surface is

$$K = \frac{\det(\mathrm{II})}{\det(\mathrm{I})}. \tag{6}$$

Example 3.3 (Curvature of the Sphere)**.** Consider the northern hemisphere of the unit sphere parameterized by

$$r(u, v) = (u, v, \sqrt{1 - u^2 - v^2})$$

and we wish to compute the Gaussian curvature at the north pole $p = (0, 0, 1)$. We have

$$r_u|_p = (1, 0, \frac{-u}{\sqrt{1 - u^2 - v^2}})|_p = (1, 0, 0)$$

and

$$r_v|_p = (0, 1, \frac{-v}{\sqrt{1 - u^2 - v^2}})|_p = (0, 1, 0).$$

We have $E = 1, F = 0$, and $G = 1$ so our first fundamental form is $\mathrm{I} = \begin{bmatrix} 1 & 0 \\ 0 & 1 \end{bmatrix}$. Our normal vector is $n(p) = (0, 0, 1)$ with

$$r_{uu}|_p = (0, 0, \frac{1 - 2u^2}{(1 - u^2)^{\frac{3}{2}}})|_p = (0, 0, 1), r_{uv}|_p = (0, 0, 0)$$

and

$$r_{vv}|_p = (0, 0, \frac{1 - 2v^2}{(1 - v^2)^{\frac{3}{2}}})|_p = (0, 0, 1).$$

Thus, $L = 1, M = 0$ and $N = 1$ and our second fundamental form is $\mathrm{II} = \begin{bmatrix} 1 & 0 \\ 0 & 1 \end{bmatrix}$ and our Gaussian curvature is $K = \frac{\det(\mathrm{II})}{\det(\mathrm{I})} = \frac{1}{1} = 1$ as expected.

We will use the first fundamental form to compute the arc length of circles on the sphere parallel to the xy plane with fixed height $z = c$ for $-1 < c < 1$. Stereographic projection, described in Section 2, allows us map our problem to the plane and perform our computations there.

Example 3.4 (Stereographic Projection Revisited[16])**.** Consider the two sphere with the north pole removed $\mathbb{S}^2 \setminus (0, 0, 1)$, stereographic projection is a bijection between the points on $\mathbb{S}^2 \setminus (0, 0, 1)$ to the $\mathbb{R}^2$. Consider a line from the north pole $(0, 0, 1)$ that intersects $(x, y, z) \in \mathbb{S}^2$ parametrized by $p(t) = (1 - t)(0, 0, 1) + t(x, y, z)$. By considering the z coordinate we determine the t value where this line intersects $\mathbb{R}^2$, namely $t = \frac{1}{1-z}$. This gives the desired map shown in Figure 3.6 and in equation form

$$p(x, y, z) \to \left(\frac{x}{1 - z}, \frac{y}{1 - z} \right).$$

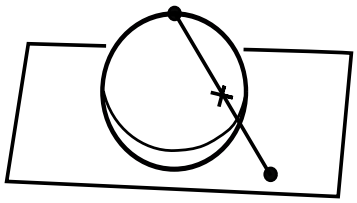

Figure 3.6: A point on the sphere is mapped to a point on the plane by stereographic projection.

The inverse is given by $p^{-1} : \mathbb{R}^2 \to \mathbb{R}^3$

$$p^{-1}(u, v) = \left(\frac{2u}{u^2 + v^2 + 1}, \frac{2v}{u^2 + v^2 + 1}, \frac{u^2 + v^2 - 1}{u^2 + v^2 + 1} \right). \tag{7}$$

To compute the first fundamental form of $p^{-1}(u, v)$ we take the partial derivatives

$$p_u^{-1} = \left(\frac{2v^2 - 2u^2 + 2}{(u^2 + v^2 + 1)^2}, \frac{-4uv}{(u^2 + v^2 + 1)^2}, \frac{4v}{(u^2 + v^2 + 1)^2} \right)$$

and

$$p_v^{-1} = \left(\frac{-4uv}{(u^2 + v^2 + 1)^2}, \frac{2v^2 - 2u^2 + 2}{(u^2 + v^2 + 1)^2}, \frac{4v}{(u^2 + v^2 + 1)^2} \right).$$

Then, after some algebra,

$$E = p_u^{-1} \cdot p_u^{-1} = \frac{4}{(u^2 + v^2 + 1)^2}$$

$$F = p_v^{-1} \cdot p_v^{-1} = \frac{4}{(u^2 + v^2 + 1)^2}$$

and

$$M = p_u^{-1} \cdot p_v^{-1} = 0.$$

We can use the first fundamental form to compute the arc length of circles on the sphere parallel to the xy plane with fixed height $z = c$ for $-1 < c < 1$. This length can be computed using the pythagorean theorem. We will see that using stereographic projection and the first fundamental form we get the same answer.

The arc length of a parameterized curve $u = u(t), v = v(t)$ on a regular surface, can be computed using the first fundamental form. Let s denote the arc length, then

$$ds = \left|\frac{dr}{dt}\right| dt = \left| r_u \frac{du}{dt} + r_v \frac{dv}{dt} \right| dt = \sqrt{(r_u^2 du^2 + 2 r_u r_v du dv + r_v^2 dv^2)}.$$

Next, use the map p to map such a circle to the plane. Using Equation 7, our circle on the sphere maps to a circle in the plane because

$$p^{-1}(u, v) = \frac{u^2 + v^2 - 1}{u^2 + v^2 + 1} = c$$

and we can compute the radius in terms of c

$$u^2 + v^2 = \frac{1 + c}{1 - c} = k^2. \tag{8}$$

In the plane, $u^2 + v^2 = k^2$ can be parameterized as

$$\gamma(t) = (k \cos(t), k \sin(t))$$

with $0 \leq t \leq 2\pi$. So our curve becomes $p^{-1} \circ \gamma(t)$ on the sphere. Computing the partial derivatives of $\gamma(t)$ gives

$$\gamma_u' = -k \sin(t) \qquad \gamma_v' = k \cos(t).$$

Now we use the first fundamental form

$$\int_{p^{-1}} \gamma ds = \int_0^{2\pi} ||(p^{-1} \circ \gamma)'(t) dt = \int_0^{2\pi} \sqrt{E(\gamma_u'(t))^2 + 2M\gamma_u'\gamma_v' + F(\gamma_v'(t))^2} dt.$$

Substituting and simplifying using $E = F$ we obtain

$$\int_0^{2\pi} \frac{2k}{k^2 + 1} dt = \frac{4\pi k}{k^2 + 1}.$$

Simplifying further using Equation 8 our arc length is

$$2\pi\sqrt{1 - c^2}.$$

Stereographic projection has the property that it preserves the angles. Maps with this property have a name.

Definition 3.1 (Conformal)**.** Let U and V be open subsets of $\mathbb{R}^n$, a function $f : U \to V$ is *conformal* at a point $u \in U$ if it preserves angles between curves through u and preserves orientation.

Proof that stereographic projection is conformal and circle preserving [31].

Theorem 3.5 (First Fundamental Form and Conformal Maps)**.** *Let S be a regular surface and $f : U \subset \mathbb{R}^2 \to V \subset S$ be a chart. Let f have first fundamental form $\mathrm{I} = Edu^2 + 2Fdudv + Gdv^2$. Then f is conformal if and only if $E = G$ and $F = 0$.*

3.2 Geodesics Curvature

Shortest paths play an important role in many computational problems. On a surface, a *geodesic* is a curve that is a shortest path between two points in the surface. For example, on $\mathbb{S}^2$ great circles are geodesic. Intuitively, the geodesic curvature of a one dimensional curve on a surface is the curvature as it would be seen from someone living on the surface.

Given a parameterized surface and a point on parameterized curve on the surface, we can compute the geodesic curvature as follows. First, find the tangent plane to the surface at the point and the unit normal vector. Let $U : \mathcal{U} \to \mathbb{R}^3$ be a parameterized chart on a surface S with vector $n(u, v)$ normal to the surface and let $\gamma(\theta)$ be a curve in U. Then $V = n(\gamma(\theta)) \times T$ is in the tangent plane of the surface since it is perpendicular to n. Moreover, $V(\theta)$ is normal to γ from the perspective of someone living on the surface. The geodesic curvature tells us the rate of change of γ' with respect to $V(\theta)$. The *geodesic curvature* is given by

$$k_g = \gamma'' \cdot (V \times \gamma'). \tag{9}$$

Example 3.6 (Circles on the Sphere)**.** We can rotate the sphere so that the circle is parallel to the xy-plane. Then the radius of the circle r is related to the height h of the circle above the xy-plane by $h^2 + r^2 = 1$. See Figure 3.7 for an example. A parameterization by arc length is given by

$$\gamma(\theta) = \left(r \cos\left(\frac{\theta}{r}\right), r \sin\left(\frac{\theta}{r}\right), \sqrt{1 - r^2} \right),$$

so

$$\gamma'(\theta) = \left(-\sin\left(\frac{\theta}{r}\right), \cos\left(\frac{\theta}{r}\right), 0 \right)$$

and

$$\gamma''(\theta) = \left(-\frac{1}{r}\cos\left(\frac{\theta}{r}\right), -\frac{1}{r}\sin\left(\frac{\theta}{r}\right), 0 \right).$$

Since we are on the sphere, the normal vector is equal to the point on the sphere so

$$n(\theta) = \left(r \cos\left(\frac{\theta}{r}\right), r \sin\left(\frac{\theta}{r}\right), \sqrt{1 - r^2} \right).$$

Then

$$k_g = \gamma'' \cdot V(\theta) = \frac{\sqrt{1 - r^2}}{r}.$$

Notice that if $h = 0$ then $r = 1$ and the geodesic curvature is zero on the equator.

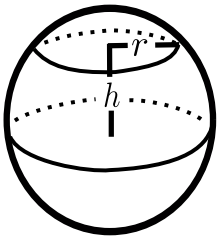

Figure 3.7: Computing the geodesic curvature.

3.3 Triangulations and The Euler Characteristic

We assume the reader is familiar with the notions of topological spaces and simplicial complexes. Most introductory topology texts describe these objects [36, 38]. The applications we will encounter will refer to triangulated surfaces in $\mathbb{R}^3$ called a *mesh*, in one application the surface will contain its interior. Each triangle in a mesh is isomorphic to a triangle in the plane and the sum of the interior angles is π.

We denote the set of vertices, edges and faces in a triangulated surface as V, E and F respectively. Let $\partial(V)$ denote vertices on the boundary of a surface and let V_{int} denote vertices that are not on the boundary. See Figure 3.8 for an example of a triangulated surface.

The *Euler Characteristic* of a surface χ is the the number of vertices minus the number of edges plus the number of faces, $\chi = |V| - |E| + |F|$. In higher dimensions, for a triangulated space X the Euler characteristic is $\chi(X) = k_0 - k_1 + k_2 - k_3 + \ldots$ where k_n is the number of simplices of dimension n. The Euler characteristic is a topological invariant of a space and does not depend on the choice of triangulation.

A graph is *planar* if it can be drawn in the plane with intersections only occurring at vertices. Two dimensional spheres $\mathbb{S}^2$ and two dimensional disk D^2 will be used in our applications. For the sphere, we have $\chi(\mathbb{S}^2) = 2$ several proofs of this can be found on David Eppstein's website [21].

We include the following proof Thurston [45]. For any planar graph we can map the graph on to the two sphere using stereographic projection.

Theorem 3.7 (Euler Characteristic for Planar Graphs)**.** *For any planar graph on the 2-sphere we have $V - E + F = 2$.*

Proof. If needed, perturb the triangulation so that the north and south poles are inside of a two faces and there are no vertical edges. At each vertex place a unit positive charge, at the center of each edge place a unit negative charge and put a unit positive charge in the middle of each face. Slam the sphere on the ground so that all charges on the edges and vertices are moved into the face below them. For faces that do not contain a pole the net charge will be zero, the northern boundary consists of an alternating sequence of edges and vertices beginning and ending with an edge. The face containing the north pole has a unit positive charge, and the face containing the south pole contains positive four units of charge and negative three units of charge. Thus, the total charge is two.

□

Triangulations of the sphere are a special case of Theorem 3.7. The sphere will be one of two common surfaces we see in applications of the Gauss-Bonnet theorem. The other being the disk. For the disk, $\chi(D^2) = 1$. This can be seen by considering the removal of a single face from a triangulation of the sphere. Once a face is removed, we can project the remaining faces of the sphere onto the plane to obtain a triangulation of a disk. Moreover, this projection is invertible and given a triangulation of a disk we can obtain a triangulation of the sphere with a single face omitted.

The Euler characteristic of a connected, orientable surface surface is often stated in terms of the genus of the surface which is defined as follows.

Definition 3.2 (Genus of a Surface)**.** The genus of a connected, orientable surface is the maximum number of cuttings along non-intersecting simple closed curves without disconnecting the surface [38].

The sphere has genus zero and the torus, shown in Figure 3.8, has genus one. For an orientable surface, the genus and the Euler characteristic are related by the formula $\chi = 2 - 2g$. To see this, we can transform a triangulation of a surface of genus g into a surface of genus $g + 1$ by removing two faces and an equal number of vertices and edges. Figure 3.9 provides an example.

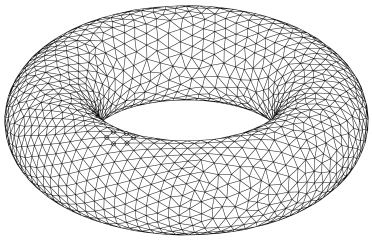

Figure 3.8: A triangulation of the torus. Image from wikipedia.

4 The Gauss-Bonnet Theorem

The Gauss-Bonnet theorem for regular surfaces states

Theorem 4.1 (The Continuous Gauss-Bonnet Theorem)**.** *If M is a regular surface with boundary ∂M then*

$$\int_M K dA + \int_{\partial M} k_g ds + \sum_i \beta_i = 2\pi\chi(M)$$

where K is Gaussian curvature, k_g is the geodesic curvature, each β_i is an exterior angle at a vertex of the boundary and χ is the Euler characteristic.

The Gauss-Bonnet theorem is telling us, if we add up curvature at each vertex the sum will be 2π times to Euler characteristic. The curvature at each vertex is computed by considering a 'local' neighborhood around the vertex and we learn global topological information. Thus,

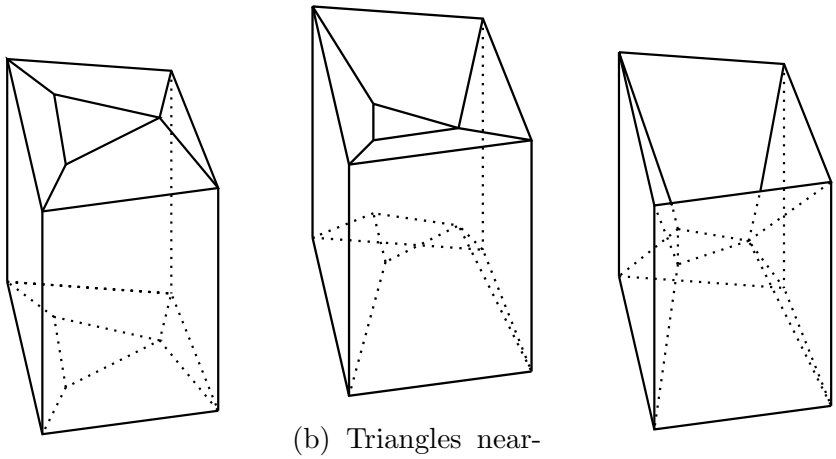

(a) Genus zero. (b) Triangles nearing. (c) Triangles join.

Figure 3.9: (a) A surface homeomorphic to the sphere with genus zero. (b) The triangle on the top and the triangle on the bottom are getting closer. (c) A surface homeomorphic to the torus. The triangle on the top and the triangle on the bottom have been removed. Three vertices and three edges have also been removed. The Euler characteristic decreased by two.

the Gauss-Bonnet theorem is an example of a local to global principle. Conversely, if we know the Euler characteristic we can learn about the curvature at individual points. We will often use the theorem to prove the existence of a vertex with a desirable amount of curvature.

4.1 Banchoff's Proof

We now include a proof of a combinatorial version of the theorem due to Banchoff [5]. We will first use another local to global theorem, the Critical Point theorem, which we now define. Given a regular surface embedded in $\mathbb{R}^3$ consider a line ℓ and define a linear height function $h : M \to \mathbb{R}$ to be the projection of all of $\mathbb{R}^3$ on to the line ℓ. A point p on M is a *critical point* for ℓ if the tangent plane at p is perpendicular to ℓ. All points on M that are not critical are *ordinary point*. Critical points can be classified into three categories, maxima, minima, and saddle points. We define the *index* of a critical point, denoted $i(p, h)$, to be $i(p, h) = 1$ if p is a local maximum or minimum and $i(p, h) = -1$ is p is a saddle point. An example is shown in Figure 4.1. The *Critical Point theorem* states that if the number of critical points is finite then

$$\sum_{p \text{ critical}} i(p, h) = \chi(M). \tag{10}$$

For an ordinary point q, the tangent plane at q is not horizontal. Now consider the plane perpendicular to ℓ and through q, this plane divides a 'small' neighborhood U of q into two pieces and intersects a 'small' circle about q in two points. Therefore, the index at a point p can be defined as follows. Let $\mathcal{C}$ denote the number of points a plane through p perpendicular

to h meets a 'small' circle around p, then

$$i(p,h) = 1 - \frac{1}{2}\mathcal{C}.$$

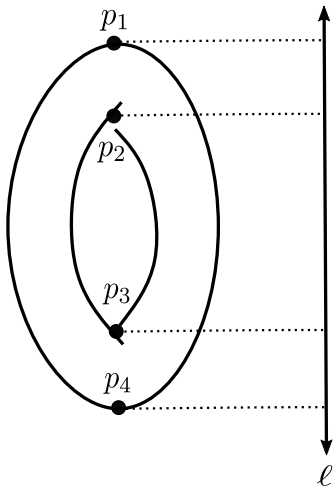

(a) The tours a line ℓ with four critical points.

(b) Local to p_1. (c) Local to p_2. (d) Local to p_3. (e) Local to p_4.

Figure 4.1: (a) A tours and line ℓ. There are four critical points. (b) The critical point p_1 is a maximum and $i(p_1,h) = 1$. (c) The critical point p_2 is a saddle and $i(p_1,h) = -1$. (d) The critical point p_3 is also a saddle and $i(p_1,h) = -1$. (e) The critical point p_4 is a minimum and $i(p_1,h) = 1$.

5 A Discrete Version

In this section, we use the Gauss-Bonnet theorem to derive a definition of discrete curvature. We discuss how discrete curvature is used to improve meshes that are generated by scanning. We then prove a discrete version of the Gauss-Bonnet theorem.

Consider a triangulated polygonal surface S with boundary $\partial(S)$. The boundary is a one dimensional piecewise linear curve in $\mathbb{R}^3$. As with polygons in the plane, at each vertex $v \in \partial(S)$ we have an exterior angle.

The interior angle might consist of many triangles. Let F_v denote the set of faces incident to v and let α_f denote the angle in face f at v. The *discrete geodesic curvature* of v is

$$k_g(v) = \pi - \sum_{f \in F_v} \epsilon_f.$$

See Figure 5.1 for an illustration. Notice that if v lies on a straight line, then $\sum_i \epsilon_f = \pi$ and the curvature is zero as we would expect.

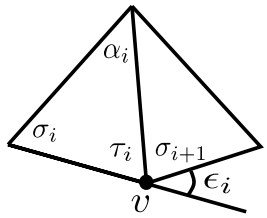

Figure 5.1: The discrete geodesic curvature at a vertex v on the boundary of a surface is given by the exterior angle ϵ.

How should be define discrete Gaussian curvature? At every non-vertex point on a polygonal surface, the continuous Gaussian curvature is zero and at every vertex it is undefined. We can use the intuitive definition of discrete geodesic curvature and the Gauss-Bonnet theorem to give a definition for discrete Gaussian curvature.

Consider removing the neighborhood around a vertex v consisting of the faces incident to v and the edges and vertices of these faces call this $N(v)$. Using the variable names given in Figure 5.1, the total geodesic curvature

$$\begin{aligned}\int_{\partial N(v)} kgds &= \sum_i \pi - (\tau_i + \sigma_{i+1}) \\ &= \sum_i \pi - (\tau_i + \sigma_I) \\ &= \sum_i \alpha_i.\end{aligned}$$

Where the second equality comes from the boundary being a circle and reorganizing the sum. Topologically, this neighborhood is a disk and $\chi(N(v)) = 1$ so the Gauss-Bonnet theorem tells us that the discrete Gaussian curvature at a vertex is

Definition 5.1 (Discrete Gaussian curvature[2])**.**

$$K(v) = \int_{N(v)} K da = 2\pi - \sum_i \alpha_i.$$

Recall, that when we considered the curvature at a vertex on a polygon in the plane in the theorem of turning tangents, Theorem 1.1, we have two parts depending on weather we use the interior or the exterior angles at each vertex. We can do a similar thing with the discrete Gaussian curvature at a vertex on a surface, instead of considering the angles of the faces incident to a vertex v, we can consider the complementary angle. The complementary

[2]Discrete Gaussian curvature is also called the *angle defect* at a vertex

angle is shown in Figure 5.2. If we let n be the number of faces incident to v, the formula for the discrete curvature then becomes

$$K(v) = 2\pi - \sum_{i=1}^{n}(\pi - \xi_i) = (2-n)\pi + \sum_{i=1}^{n}\xi_i. \tag{11}$$

By Equation 2, this is the area of the polygon on the sphere with interior angles $\xi_1, \xi_2, \ldots \xi_n$. Geometrically, this angle be seen in Figure 5.2. If we project the normal vectors on each face onto a sphere and connect these points with great arcs to create a polygon on the sphere with interior angles $\xi_1, \xi_2, \ldots \xi_n$. We have a geometric representation of discrete Gaussian curvature as the area on the unit sphere bounded by a spherical polygon whose vertices are the unit normals of the faces around v. An example is shown in Figure 5.3.

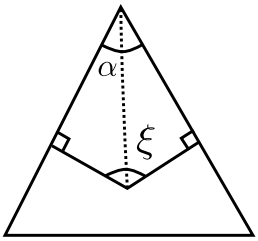

Figure 5.2: The relationship between the angles incident to a vertex and its complementary angle.

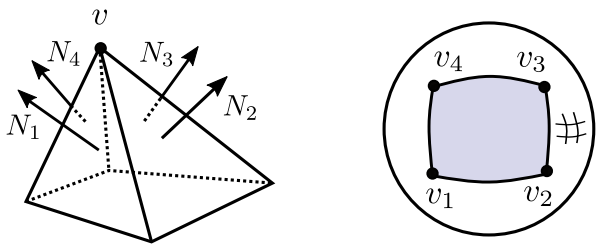

Figure 5.3: Consider the vertex v in the figure on the left. The curvature of v is the area on the sphere shown on the right. We rotated the sphere in order to see the entire polygon.

Combining the above definitions we have

Theorem 5.1 (The Discrete Gauss-Bonnet Theorem)**.** *If S is a triangulated surface with boundary ∂S then*

$$\sum_{v \in V_{int}} K(v) + \sum_{v \in V_{\partial S}} k_g(v) = 2\pi\chi(S)$$

where $K(v)$ is the discrete Gaussian curvature of a vertex, $k_g(g)$ is the discrete geodesic curvature, and χ is the Euler characteristic.

5.1 Reducing the Size of a Mesh

The definition of discrete Gaussian curvature that we derived by applying the Gauss-Bonnet theorem is used when a triangulated surface is generated by scanning an object. In this context, a triangulated surface is called a mesh.

Meshes that are obtained by scanning real objects contain noise. Most meshes that are generated by scanning require a complete remeshing [1]. As a first step in remeshing, the curvature at each vertex needs to be estimated [37].

Computing the curvature at each vertex in a mesh can allow one to reduce the number of vertices in the mesh without sacrificing mesh quality. This leads to simplification process that reduces storage space and improves the efficiency of algorithms run on the mesh. If the curvature at a vertex is zero, then the vertex can be removed, along with the faces and edges incident to the vertex, without changing the mesh. If the curvature is small, then few points are sampled to be included in the re-mesh. If the curvature is large, then many points are sampled. See Figure 5.4 for an illustration.

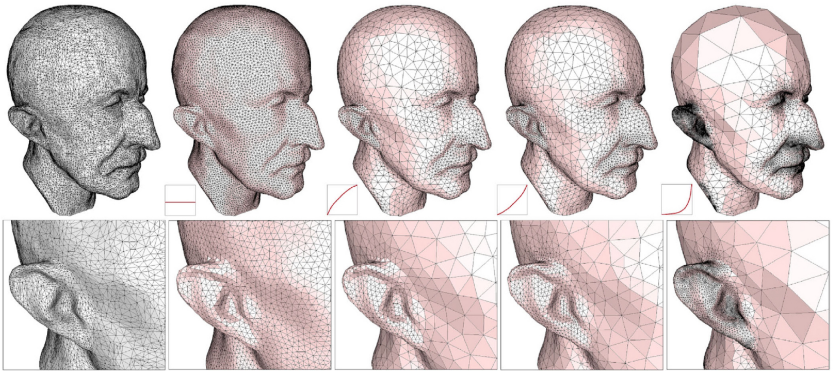

Figure 5.4: A mesh of Max Plank. The original mesh is on the left. As we move from left to right more importance is placed on vertices with large curvature. Figure from [2].

The experiments in [37] found that the average percent error did not exceed 1.3% when using this operator.[[**XXX TODO:** what does this mean?]]

5.2 A Combinatorial Proof

We present a proof of the Gauss-Bonnet theorem similar to the proof given by Upadhyay [47]. First, we consider the case where our surface does not have a boundary. We then extend this case to surfaces with boundary.

Theorem 5.2 (Discrete surfaces without boundary)**.** *For a triangulated surface S without boundary*

$$\sum_{v \in V} K(v) = 2\pi\chi(S)$$

where $K(v)$ is the discrete curvature.

Proof. For each vertex v in S, let $deg(v)$ denote the number of edges incident to v, let $\alpha_1, \alpha_2, \ldots, \alpha_{\deg(v)}$ denote the angles containing v and let $\xi_i = \pi - \alpha_i$ for each i. By Equation 11, the discrete Gaussian curvature at a v is

$$K(v) = (2 - \deg(v))\pi + \sum_{i=1}^{\deg(v)} \xi_i.$$

Summing over all vertices in S gives

$$\sum_{v \in V} K(v) = \sum_{v \in V} 2\pi - \sum_{v \in V} \deg(v)\pi + \sum_{v \in V} \sum_{i=1}^{\deg(v)} \xi_i.$$

The first term on the right hand side is $2\pi|V|$. Each edge is incident with two vertices, so the second term is $2\pi|E|$. In the third term, we rewrite ξ_i as $\pi - \alpha_i$.

$$\sum_{v \in V} \sum_{i=1}^{\deg(v)} \beta_i = \sum_{v \in V} \sum_{i=1}^{\deg(v)} (\pi - \alpha_i).$$

We can reorganize this sum as follows, instead of summing the angles around each vertex we can sum the angles in each face. Each angle in S is still being counted exactly once. Since each face is a triangle, this gives

$$\sum_{v \in V} \sum_{i=1}^{\deg(v)} (\pi - \alpha_i) = \sum_{f \in F} \sum_{i=1}^{3} (\pi - \alpha_i).$$

Since each face is a triangle the sum of the three angles is π, so $\sum_{i=1}^{3}(\pi - \alpha_i) = 3\pi - \pi = 2\pi$. Thus,

$$\sum_{v \in V} K(v) = 2\pi|V| - 2\pi|E| + 2\pi|F| = 2\pi\chi(S)$$

as desired. □

Next, we extend the above proof to the case where S has a boundary by gluing a copy of S to itself along the boundary.

Theorem 5.3 (Discrete surfaces without boundary)**.** *For a combinatorial surface S with boundary*

$$\sum_{v \in S_{int}} K(v) + \sum_{v \in \partial S} k_g(v) = 2\pi\chi(S)$$

where $K(v)$ is the discrete curvature and $k_g(v)$ is the discrete geodesic curvature.

Proof. Take a copy of S and attach it to itself along the boundary. This creates the surface $2S$ without boundary. Notice, when we copy S we create two copies of the boundary, and when we glue we remove one copy of the boundary. Thus,

$$\chi(2S) = 2\chi(S) - \chi(\partial S).$$

Since, ∂S is piecewise linear the number of vertices and edges are equal and there are no faces, so $\chi(\partial S) = 0$ and

$$\chi(2S) = 2\chi(S). \tag{12}$$

For v a vertex on the boundary, $k_g(v)$ is half the discrete Gaussian curvature of v in $2S$. Thus,

$$\sum_{v \in 2S} K(v) = 2\left(\sum_{v \in S_{\text{int}}} K(v) + \sum_{v \in \partial S} k_g(v)\right) = 2\pi\chi(2S).$$

Applying Equation 12,

$$\sum_{v \in S} K(v) + \sum_{v \in \partial S} k_g(v) = 2\pi\chi(S)$$

as desired.

□

6 Applications

6.1 The Harry Ball Theorem

Functions on surfaces are called vector fields. In this section, the Gauss-Bonnet theorem is used to relate the zeros of a vector field to the topology of a surface. We will prove that harry ball theorem which shows that given a harry ball, one can not comb the ball without creating a cowlick.

Definition 6.1 (Vector Field)**.** A vector field v on an open set $U \subset S$ of a regular surface S is a correspondence which assigns a vector $w(p) \in T_p(S)$ to each $p \in U$. Moreover, v is differentiable at p if, for some parametrization $r(u, v)$ at p, the functions $a(u, v)$ and $b(u, v)$ given by

$$v(p) = a(u, v)r_u + b(u, v)r_v$$

are both differentiable at p.

A point $p \in S$ in vector field is a *singular point* if $v(p) = 0$ moreover, a singular point is *isolated* if there is an open neighborhood containing p and no other singular points. These, and the following definition, extend to higher dimensions.

Let $f : \mathbb{S}^n \to \mathbb{S}^n$ be a continuous map. Let $H_n(\cdot)$ dentote the nth homology group, then f induces a homomorphism $f_* : H_n(\mathbb{S}^n) \to H_n(\mathbb{S}^n)$ and $H_n(\mathbb{S}^n) \cong \mathbb{Z}$. Every homomorphism from $\mathbb{Z}$ to itself is of the form $f_* : n \mapsto kn$ for some $k \in \mathbb{Z}$ the integer k is the *degree* of the map f.

Isolated singular points give a map from the circle to itself. Let σ be a circle surrounding a singular point p. Since $v(p)$ is isolated we can choose the radius of σ to be small enough so that $v|_\sigma \neq 0$. The *index* of a isolated critical point p of v is the degree of the map $f : \sigma \to \mathbb{S}^1$ where$f(p) = v(p)/||v(p)||$.

Theorem 6.1 (Poincaré-Hopf Theorem)**.** *Let S be a closed and bounded regular surface and let v be a vector field on S such that every zero of v is isolated. If S has a boundary, then assume v is outward normal on the boundary. Then*

$$\sum_i I(v_i) = \chi(S)$$

where v_i denotes the set of isolated zeros.

We now prove that given a ball with a hair attached to each point, you can not comb the ball without creating a cowlick.

Theorem 6.2 (The Harry Ball Theorem)**.** *Let v be a vector field on the sphere $\mathbb{S}^2$. Then there is a $p \in \mathbb{S}^2$ such that $v(p) = \vec{0}$.*

Proof. For a contradiction, assume that $v(p) \neq 0$ for all $p \in \mathbb{S}^2$, this would give a vector field on $\mathbb{S}^2$ with no singular points. However, the Euler characteristic of $\mathbb{S}^2$ is two and Theorem 6.1 implies that any vector field on $\mathbb{S}^2$ has at least two isolated singular points.

□

[43]

6.2 Robotics

In may 2023 I asked chatgbt to give me some applications of the Gauss-Bonnet theorem and returned that there were applications to robotics. I asked for some references it gave me references that were made up. But the suggestion lead me to the following not made up application of the Gauss-Bonnet theorem in robotic route planning is given by K.-L. Wu et. al. in [49]. Suppose have a robot navigating a 3D[[**XXX TODO:** 2 or 3 manifold?]] terrain with a single obstacle and we wish to plan trips for our robot. In this application, a terrain is a smooth manifold [[**XXX TODO:** not defined]] with tangent planes at every point. An obstacle is modeled by a hazardous ball with a grade depending on the radius. Assume that checking if a path intersects the obstacle can be done in constant time.

Overview of their procedure. We are given two points s and t on a ?-manifold M. First, compute a geodesic path from s to t call this path $\gamma(x)$. If the γ does not intersect the obstacle we are done. Otherwise, the γ intersects the obstacle we call the initial intersection point between our path and the boundary of the obstacle p. Construct the tanged plant TpM at p. Choose a vector $v \in TpM$ and a value α for the magnitude of v. Next, define two points α_ℓ and α_u to be in the directions of v and $-v$ at a distance of α from p in the tangent plane. Then project the points α_ℓ and α_u onto the surface? to obtain the points q and r. We next compute four new geodesics $g_1(s)$ from s to q, $g_2(s)$ from q to t, $f_1(s)$ from s to r and $f_2(s)$ from r to t. Let $\gamma_g = g_2 \circ g_1$ and $\gamma_f = f_2 \circ f_1$.

We then use the Gauss-Bonnet theorem to decide which alternative path is best. If the edges of a triangle are all geodesic then we have a *geodesic triangle* $\tau \subset M$. We have two geodesic triangles, γ, g_1, g_2 and γ, f_1, f_2.

Here we have cusps at the intersection points of the geodesics, to account for this, our Gauss-Bonnet is

$$\int\int_\tau K dA + \sum_{i=1}^{3}(\pi - \theta_i) + \sum_{i=1}^{3}\int k_g ds = 2\pi \tag{13}$$

where θ_i are the interior angles of τ. Since we are on geodesics $\int k_g ds = 0$ and we can rearrange Equation 13 to obtain

$$\theta_1 + \theta_2 + \theta_3 = \pi + \int\int_\tau K dA. \tag{14}$$

We can estimate the curvature based on the sum of the angles of $\sum_{i=1} 3\theta$. They show that f $K = 0$ on τ then γ_f and γ_g are identical and there exists an α^* that makes them shortest. If $\sum_{i=1}^{3}\theta_i > \pi$ then is $\int_? K > 0$ on all of τ then and if $\sum_{i=1}^{3}\theta_i < \pi$ then $K < 0$ on (average) all of τ. The authors state that we should avoid negative curvature because it is "energy-consuming ascending and descending motions required" and would require the robot have "better mobility and maneuverability". [[**XXX TODO:** I don't see why]].

6.3 How Many Deltahedron Exist?

In this section, we share a proof due to Fushsida-Hardy [24] that there are only eight deltahedron. A *deltahedron* is a polyhedron whose faces are all equilateral triangles. Two examples are shown in Figure 6.1.

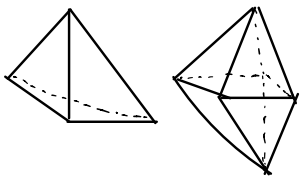

Figure 6.1: Two deltahedron. A tetrahedron and an octahedron.

How many convex deltahedron are there? Any convex deltahedron is homeomorphic to the sphere. So we know $\chi(S) = 2$ and there is no boundary.

Let $T = (V, E, F)$ be a triangulation of the sphere. We will used a modified statement of the Gauss-Bonnet theorem. Since equilateral triangles are perimeter minimizing triangles, the ratio of perimeter to diameter is 3 not π. Again due to equilateral triangles, the curvature of a vertex is $K(v) = 6 - deg(v)$.

Then, the Gauss-Bonnet theorem states,

$$\sum_{v \in V} K(v) = 2 \cdot 3 \cdot 2.$$

Since we have a triangulation each vertex must have degree at lease three. Thus, $K(v) \leq 3$ for all v. But, since we have convex faces, $K(v) \geq 1$ for all v.

So, for $1 \leq k(v_i) \leq 3$ and $\sum k(v_i) = 12$, so we only need to examine a finite number (19) of cases. For example, if the curvature at each vertex is three then, we have four vertices. Each vertex is incident to three edges and each edge has two vertices so $\frac{3}{2}4 = E = 6$ and there are four faces. This is the tetrahedra.

6.4 Pseudosphere

In this section, we share a proof due to [10] that the Euler characteristic of the pseudosphere is zero.

Define the tractrix, a bike with front wheel on the x-axis going from negative infinity to positive infinity, the back wheel is moving backwards while the front wheel is on the negative x-axis then the back wheel switches to roll forward when the front wheel is on the positive x-axis. The path of the back wheel is the tractrix.

The pseudosphere is the surface formed by rotating the tractrix around the x-axis. The paper rigoursly proves that the pseudosphere has constant Gaussian curvature of negative one and area of 4π.

The geodesic curvature along the boundary of the truncated (at $x = 0$ and $x = a$ a approches infinity) which turns out to be 2π. We then plug into the Gauss-Bonnet to determine that the Euler characteristic of the top half of the pseudosphere is zero! This implies that that the half-pseudosphere is homeomorphic to the cylinder.

[[**XXX TODO:** isn't this obvious from the fact that we are truncating the pseudosphere?]]

6.5 Triangulating Noncovex Polyhedra

A three-dimensional solid with polygonal faces and straight edges is called a *polyhedra*. We often wish to decompose a polyhedra into tetrahedra much like we decompose polygons into triangles. Moreover, we would like to represent a polyhedra with as few tetrahedra as possible [30].

A polyhedron is *simple* if it is homeomorphic to the sphere and the faces are all polygons. Let P be a a simple polyhedron with n vertices. In [12], Chazell uses the Gauss-Bonnet theorem to show that, in the worst case, decomposing the P into tetrahedra requires $\Omega(n^2)$ tetrahedra.

An edge e in P is *reflex* if the interior angle formed by its two incident faces is greater than π. See Figure 6.2 for an example. A vertex is reflex is it is incident to a reflex edge. Let r denote the number of reflex edges.

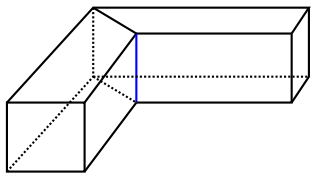

Figure 6.2: A polyhedron with one reflex edge (blue), the two vertices incident to the blue edge are reflex vertices.

Chazell and Palios give an algorithm to triangulate a nonconvex simple polyhedra [11]. Their algorithm creates a refinement with $O(n + r^2)$ tetrahedra in $O(n \log r + r^2 \log r)$ time and $O(n + r^2)$ space. The algorithm first removes $n - 4r$ non-reflex or flat vertices to create a representation of the polyhedra with $O(r)$ vertices. Then, vertical planes decompose the reduced polyhedra in to $O(r^2)$ convex cells.

Chazelle and Shouraboura use the Gauss-Bonnet theorem to show any polyhedron of genus g must have at least $g - 1$ reflex edges [13]. This implies that any polyhedron can be decomposed with $O(n+r^2)$ tetrahedra, regardless of the genus! We present their application.

In this application, to simplify computation, we scale the curvature of a vertex by $\frac{1}{2\pi}$, so $K(v) = \frac{1}{2\pi}(2\pi - \sum_i \alpha_i)$, We relate the number of reflex edges incident to a vertex v to $K(v)$.

Lemma 6.3. *The number of reflex edges incident to a vertex v is at least $-K(v)$.*

Proof. For each vertex, center a sphere at the vertex, see Figure 6.3a. The intersection of the polyhedron and the sphere gives a 'polygon' on the sphere with boundary L consisting of great circles. Scale the sphere to have unit radius. Then, the length of each arc in L is equal the the angle incident to v, so the total length of L is the sum of the angles incident to v, see Figure 6.3.

Let R be the number of reflex edges incident to v. If R is zero, then P is convex at v and has non-negative curvature so $0 > -K(v)$. If $R > 0$, reflex edges incident to v correspond to reflex angles on L. For each reflex angle, bisect it and reduce the number of reflex angles and obtain a decomposition of the sphere into at most $R+1$ convex regions, thus $L \leq 2\pi(R+1)$.

Thus, we have $L = \sum \alpha_f$ and the curvature $K(v) = 1 - \frac{1}{2\pi} \sum \alpha_f$ giving $L = 2\pi(1 - K(v))$. Combining this with $L \leq 2\pi(R+1)$ gives $-K(v) \leq R$.

□

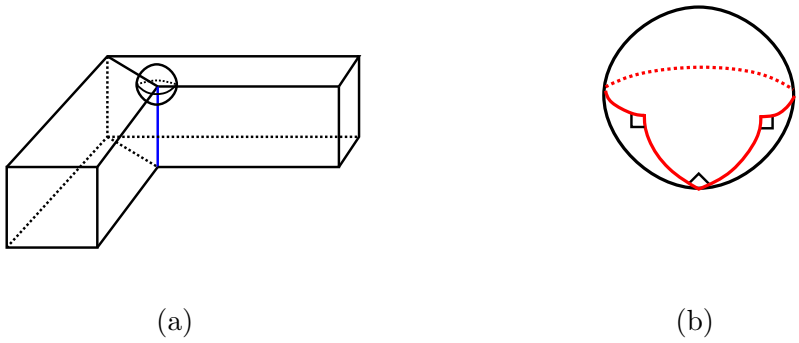

(a) (b)

Figure 6.3: (a) A sphere centered at a reflex vertex. (b) The 'polygon' of great circles where the polyhedron intersects the sphere.

Next, we show

Theorem 6.4 (Reflex Angles)**.** *Any polyhedron of genus g must have at least $g-1$ reflex dihedral angles.*

Proof. Let r be the total number of reflex edges in a polyhedra. By the classification of oriented surfaces, the Euler characteristic is determined by the genus, $\chi = 2 - 2g$. By Lemma 6.3, $\sum_v -K(v) \leq 2r$ since each reflex edge is incident to two vertices. By the Gauss-Bonnet theorem $\sum_v K(v) = 2 - 2g$, so $-2r \leq 2 - 2g$ and $g \leq r + 1$ as desired.

□

Given a polyhedron of genus g, we can temporally duplicate the vertices around each essential cycle and insert disks, creating a polyhedron of genus zero, we then apply the algorithm to decompose genus zero polyhedra given in [11]. Then remove the added disks. Since we added g disks the algorithm decomposes the polyhedron into $O(n + (r+g)^2)$ tetrahedra. By Theorem 6.4, $g \leq r + 1$ showing that the upper bound on the number of tetrahedra in a triangulation of a polyhedra is $O(n + r^2)$ regardless of the genus.

6.6 Digital Topology

In two dimensions, a black and white image consists of an array of pixels where each pixel is either black or white. In three dimensions, instead of square pixels we have cubes called voxels. Three dimensional images are use useful in medical images. For example, consider a three dimensional images of the human heart [9]. Given such an image, one might want to compute the number of holes in the image to make sure it matches the number of holes that are suppose to be in the human heart. In this subsection, we share a result of Chen and Rong where they use the Gauss-Bonnet theorem to compute genus of a digital image

in $\mathbb{R}^3$ [14]. In most of our other uses of the Gauss-Bonnet theorem we begin with surface where we know the Euler characteristic, the sphere or the disk, and use the theorem to tell us about the local curvature. In this application, we are going in the opposite direction, we are using the local curvature to compute the genus.

Digital images are commonly reffered to as *cubical complexes*, where each cube has side length one [33]. An *elementary cube* Q is a product

$$Q = I_1 \times I_2 \times I_3$$

where each I_i is a unit interval of the form $I = [\ell, \ell + 1]$ called a *coordinate*. We will often associate each elementary cube with a lattice point see Figure 6.4 for an example.

Our goal is to use the Gauss-Bonnet theorem to compute the genus of a three dimensional cubical complex. The definition of genus, Definition 3.2, is given in terms of simple closed curves. In order to describe a closed curve in a cubical complex we first need to resolve an interesting paradox. In two dimensions, it is not clear what it means for two pixels to be adjacent. For example, in Figure 6.4a we see four black pixels. Should these pixels represent a closed curve? If we define the pixels adjacent to a given pixel to be the pixels to the left, right, above, and below, then each black pixel isolated and the four pixels should not form a closed curve. However, with adjacency defined this way, the white pixel in the middle is completely surrounded and the four black pixels should represent a closed curve because they separate the white pixels into an inside and an outside. In order to resolve this paradox introduce different notions of adjacency.

In two dimensions, two points are *eight-adjacent* if they are distinct and each coordinate of one differs from the other by at most one. Two points are *four-adjacent* if they are eight-adjacent and differ in at most one of their coordinates. Consider four vertices adjacent to a single vertex v.

Returning to our paradox in Figure 6.4a. If we use eight-adjacency for the white vertices and four-adjacency for the black. Then the four black pixels do not form a closed curve and the center white pixel is not enclosed, so we avoid our paradox. Notice we could have chosen four adjacency for the white vertices and eight-adjacency for the black pixels and now the four black pixels do form a closed curve and the white pixel is surrounded and again we do not have a paradox.

We make a similar choice in three dimensions, two points are *26-adjacent* if they are distinct and each coordinate entry differs by at most one. The points are *18-adjacent* if they are 26-adjacent and different in a most two of their coordinates. The points are *6-adjacent* if they are 18-adjacent and differ in at most one of their coordinates. If a set of points S lattice points cannot be partitioned into two subsets that are not n-adjacent is *n-connected*.

A *digital picture* is a quadruple (V, m, n, B) where $V = \mathbb{R}^2$ and $(m, n) = (4, 8)$ or $V = \mathbb{R}^3$ and $(m, n) = (6, 26)$ and B is a subset of V. Elements of B are black vertices and elements not in V are white.

One may ask, why don't we triangulate the cubical complex and count vertices, edges, and faces to determine the genus. One reason against doing this is that decomposing a cubical complex into a simplicial complex results in 24 times as many highest dimensional cells [32].

The objects we wish to compute the genus of are closed, orientable, cubical complexes

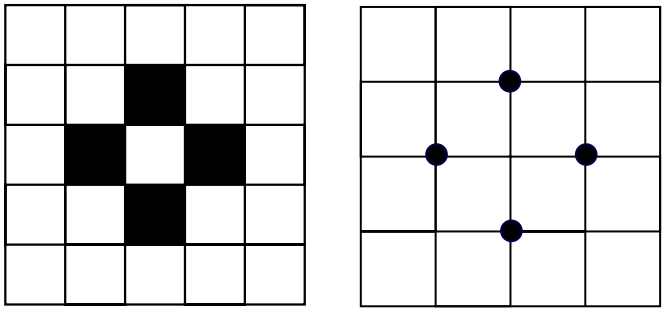

(a) (b)

Figure 6.4: (a) A two dimensional image with four black pixels. Do the black pixels represent a closed curve? (b) The same image represented on the lattice.

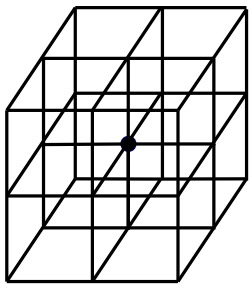

Figure 6.5: A vertex in a three dimensional cubical complex and its 26 neighbors.

in $\mathbb{R}^3$ with $(6, 26)$-connectivity. If M is such a complex, there are six types of digital surface points, these are shown in Figure 6.6.

Let M_i denote the set of digital points with i neighbors and K_i the curvature. Then, by Definition 5.1, we compute the discrete curvature at each of this points to obtain

(a) $K_3 = \pi/2$,

(b) $K_4 = 0$,

(c) $K_5 = -\pi/2$,

(d) $K_6 = -\pi$.

Then, by the Gauss-Bonnet theorem, we have

$$\sum_{i=3}^{6} K_i |M_i| = 2\pi(2 - 2g).$$

A linear time algorithm to compute the genus is the following. Iterate through all points in M and count the neighbors at each point and keep track of M_i. Then calculate the genus by rearranging the above equation to obtain

$$g = 1 + (|M_5| + 2|M_6| - |M_3|)/8.$$

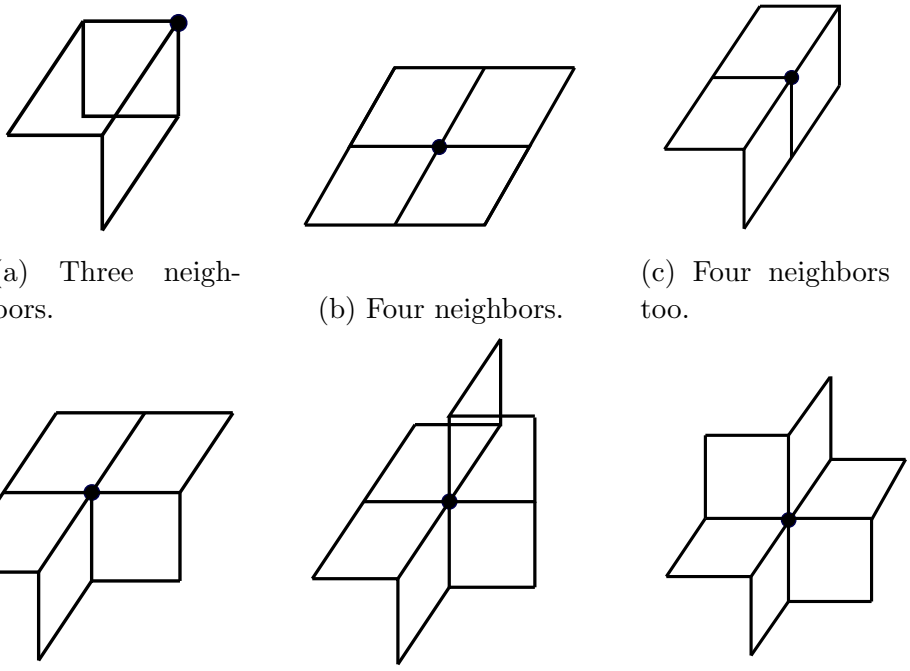

(a) Three neighbors. (b) Four neighbors. (c) Four neighbors too.

(d) Five neighbors. (e) Six neighbors. (f) Six neighbors too.

Figure 6.6: This six types of digital surface points.

6.7 Homotopy Testing

Homotopy classes of curves are important because... In this section, we share applications where the Gauss-Bonnet theorem is used to determine if curve on a surface is contractible. An explanation of this algorithm is given in a video lecture by Jeff Erickson [22].

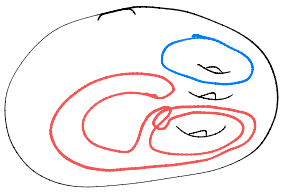

Figure 6.7: The blue curve is not contractable, the red curve is contractable.

In this application, we will use a modified version of the Gauss-Bonnet theorem. Given a combinatorial surface S define the curvature of a face to be $k(f) = 1 - \sum \beta_f$, $k(v) = 1 - \frac{1}{2}\deg(v) + \sum_{v \in V} \alpha_v$. Summing over all faces and vertices in S gives,

Theorem 6.5 (Modified Gauss-Bonnet)**.** *For a combinatorial surface S, $\sum_{f \in F} k(f) + \sum_{v \in V} k(v) = \chi(S)$.*

Proof.

$$\sum_{f\in F} k(f) + \sum_{v\in V} k(v) = |F| - \sum_{v\in V} \alpha_v + |V| - |E| + \sum_{v\in V} \alpha_v = \chi(S).$$

□

Here, a we have a combinatorial surface that we call a map denoted S with genus $g \geq 2$. The case $g = 0$ is the sphere where every curve is contractible and when $g = 1$ contractibility can be determined by a counting argument[[**XXX TODO:** explain]]. A curve is a closed walk, given as alternating sequence of vertices and edges in S. A *homotopy* between two closed curves γ_1 and γ_2 that share a point p_0 is a continuous map $H\colon [0,1] \times \mathbb{S}^1 \to \mathbb{R}^2$ such that $H(0,\cdot) = \gamma_1$, $H(1,\cdot) = \gamma_2$, and $H(s,0) = p_0 = H(s,1)$.

On a combinatorial surface, homotopies can be decomposed into discrete moves called edge spikes, edge unspikes and face flips. The question we consider is: Given a closed walk W in a map Σ is there a finite sequence of moves that reduces the curve to a trivial walk?

First, we transform S into a simpler object called a system of loops. Let T be a spanning tree of S, let C be the edges in a co-tree (a spanning tree of the dual), and let L denote the left over edges, Each edge in S is in one of (T, L, C). Contract edges in T, delete edges in C a system of loops Δ. When we contract and delete edges in S we might affect edges in our walk W. If we contract an edge in W, delete the edge from W. If we delete and edge $e \in W$, face flip to avoid the deleted edge. Get a new walk $W' \in \Delta$ homotopic to $W \in \Sigma$ now only haveing one vertex. Then, W' has one vertex with degree $4g$, one face with $4g$ edges, and $2g$ loops. The length of the walk increases by at most $2g$.

The universal covering space of S denoted U is a plane and when $g \geq 2$ U has a natural hyperbolic geometry, tiled by $4g$-gons.

Big idea: a curve is contractible closed walk in S if and only if the walk is closed U. Thus, our problem is equivalent to the following: Given a walk in the universal cover of a system of loops, is it closed?

Here the walk is given as a starting vertex then we have a list of which edges to take at each intermediate vertex. All vertices look the same, so we must determine if we have ended where we began.

Look for spurs or taking and instances where we talk the long way around a face, shorten the walk. Any nontrivial contractible cycle contains either a spur or a bracket [6].

Lemma 6.6 (Dehn's Lemma)**.** *If $g \geq 2$, then any nontirival closed walk has either a spur or $4g - 2$ consecutive edges on the boundary of a face.*

Proof. Sketch: Any nontrival closed walk bounds a disk D with $\chi(D) = 1$, by the Gauss-Bonnet theorem

$$\sum_{v} k(v) + \sum_{f} k(f) = 1.$$

Each face has $4g$ edges, each internal vertex has degree $4g$ and each boundary vertex has degree less than $4g$. The angle of each angle on a face is $\frac{1}{4}$, thus, $k(f) = 1 - g < 0$, for internal vertices $k(v) = 1 - g < 0$ and for all vertices on the boundary, $k(v) = \frac{3}{4} - \frac{\deg(v)}{4}$. Boundary vertices fall into three categories: convex, where $k(v) = \frac{1}{4}$ flats, where $k(v) = 0$ and concave where $k(v) < 0$.

By G-B,

$$|F|(1-g) + |v_{convex}|\frac{1}{4} \geq 1$$

and

$$|v_{convex}| \geq (4g-4)|F| + 4.$$

We divide by $|F|$ to determine the average number of convex vertices per face to be greater than $4g-4$. Thus, there exists some face that has $4g-3$ consecutive edges in the walk. □

This gives an algorithm for determining if a walk is closed in the universal covering space. Look for spurs and long boundary subpaths, the walk is closed if and only if we can shrink the curve. Label edges, walk is a sequence of labels look at intervals of $4g-2$ in a walk, $8g$ paths that represent long boundary paths, $4g$ spurs. Slide window and look for spurs or long boundary paths. If you find one remove it.

Brute force $O(g^3\ell)$ overall. Can speed it up with Erickson DFA idea $O(g^2 + g\ell)$. Overall runtime $O(n + g^2 + g\ell)$ time.

In trouble if $g$is big. Erickson uses system of quads, radial map, $O(n)$ runtime [23].

6.8 The Fundamental Theorem of Algebra

In this section, we share a proof due to Almira and Romero that the Gauss-Bonnet theorem implies the Fundamental Theorem of Algebra [3]. The theorem is the following:

Theorem 6.7 (Fundamental Theorem of Algebra)**.** *Let $f : \mathbb{C} \to \mathbb{C}$ be a non-constant single-variable polynomial with complex coefficients, then f has a least one complex root.*

We now include standard ideas and definitions from complex analysis that are used in the proof. A complex number represented $z = x + iy$ where x and y are real and $i^2 = -1$. A continuous complex function is a map $f : \mathbb{C} \to \mathbb{C}$ we often write $f(z) = f(x, y) = u(x, y) + iv(x, y)$ where u is called the real part and v is the imaginary part. The derivative of a complex function is defined similalry to the derivative of a real valued function via a limit. The *derivative* of f at z_0 is

$$f'(z_0) = \lim_{h \to 0} \frac{f(z_0 + h) - f(z_0)}{h}$$

if the limit exists and is undefined if the limit does not exist. Many of the differentiation rules from calculus apply to complex function, in particular the sum and power rules apply. Thus, it is straightforward to to take derivatives of polynomials.

A function f is *analytic* at a point z_0 if there exists a neighborhood around z_0 such that f is differentiable at each point in the neighborhood. We will see that the fact that f has a derivative in a domain tells us a lot about the function. For instance, analytic functions satisfy the Cauchy-Riemann equations meaning

$$\frac{\partial u}{\partial x} = \frac{\partial v}{\partial y} \text{ and } \frac{\partial u}{\partial y} = -\frac{\partial v}{\partial x}.$$

The Cauchy-Riemann equations give a way to test for analyticity, if the equations are satisfied then the function is analytic. The equations give a convenient way to compute the derivative, namely

$$f'(z) = \frac{\partial u}{\partial x} + i\frac{\partial v}{\partial x} = \frac{\partial v}{\partial u} - i\frac{\partial u}{\partial y}.$$

The *Laplacian* of a function is the sum of the second order partial derivatives, denoted Δf, or just Δ if the function is clear, in our case, $\Delta f = \frac{\partial^2 f}{\partial x^2} + \frac{\partial^2 f}{\partial y^2}$. The equations

$$\frac{\partial^2 u}{\partial x^2} + \frac{\partial^2 u}{\partial y^2} = \frac{\partial^2 v}{\partial x^2} + \frac{\partial^2 v}{\partial y^2} = 0$$

are call Laplace's equation and are one of the most famous equations in applied mathematics [50]. A function that satisfies Laplace's equation is said to be *harmonic*.

We will use of the following lemma

Lemma 6.8 (Analytic Implies Real Part Harmonic)**.** *The real part of an analytic function is harmonic.*

Proof. Since our function is analytic, the Cauchy-Riemann equations are satisfied. Differentiating again and using the fact that the mixed partial derivatives are equal, we have

$$\frac{\partial^2 u}{\partial y^2} = -\frac{\partial}{\partial y}\left(\frac{\partial v}{\partial x}\right) = -\frac{\partial}{\partial x}\left(\frac{\partial v}{\partial y}\right) = -\frac{\partial^2 u}{\partial x^2}.$$

And

$$\frac{\partial^2 u}{\partial x^2} + \frac{\partial^2 u}{\partial y^2} = 0.$$

□

We will need a fact about the complex logarithm function, to this end the *complex exponential function* is defined to be

$$e^z = e^x \cos(y) + ie^x \sin(y).$$

This function has many desirable properties: it is differentiable everywhere, it is equal to its own derivative, it agrees with the real exponential when the input is restricted to the reals, and satisfies the same algebraic properties of the real exponential such as

$$e^{z_1+z_2} = e^{z_1}e^{z_2}.$$

When we write the function in polar form we see that

$$|e^z| = e^x \qquad \text{and} \qquad \arg(e^z) = y + 2\pi n$$

for $n \in \mathbb{Z}$. The complex exponential differs from the real exponential in that it is periodic with a imaginary period of $2\pi i$. This is significant because we wish to define the inverse. The infinite horizontal strip

$$-\infty < x < \infty, \qquad -\pi < y \leq \pi$$

is the *fundamental region.*

Now to define the complex logarithm. Let $\log_e(x)$ denote the real logarithm. Suppose

$$e^w = z,$$

then $|e^w| = |z|$ and $\arg(e^w) = \arg(z)$. Then $u = \log_e |z|$ and $v = \arg(z)$ and we have

$$\ln(z) = \log_e |z| + i \arg(z).$$

Notice that since there are an infinite number of arguments for z, the logarithm gives infinitely many values but there is only one value in the fundamental region. And now the fact about the complex logarithm that we will need in the proof of Theorem 6.7.

Lemma 6.9 (Complex Logarithm Fact)**.** *For any complex function $f(z)$ we have*

$$\ln(|f(z)|) = \boldsymbol{Re} \ln(f(z)).$$

Proof. This fact follows from the definition of the complex logarithm. The modulus $|f(z)|$ is a real number and so $\ln(|f(z)|) = \log_e(|f(z)|)$. On the other hand, $\ln(f(z)) = \log_e(|f(z)|) + i \arg(f(z))$ and so $\mathbf{Re} \ln(f(z)) = \log_e(|f(z)|)$. □

The proof of Theorem 6.7 requires one additional idea. We now show that if we apply a conformal diffeomorphism to a surface of constant curvature we can calculate the curvature of the resulting surface. This result is often referred to as Liouville's equation [17, 20, 35].

Let $f : S \to S$ be a conformal differentiable map with local coordinates $f(u, v)$. Such maps do not necessarily preserve geometric measurements (curvature or area), but the change can be accounted for. The first fundamental form tells us how the area changed by f

$$d\ell^2 = Edu^2 + 2Fdudv + Gdv^2.$$

Since our map is conformal, we can apply Theorem 3.5, and we know $E = G$ and $F = 0$ and

$$d\ell^2 = Gdu^2 + 0dudv + Gdv^2 = G(du^2 + dv^2).$$

We call $g(u, v) = G$ the *induced metric* of f.

Theorem 6.10 (Liouville's Theorem)**.** *Let $f(u, v)$ be conformal coordinates of a surface with constant curvature $S \subset \mathbb{R}^3$ with induced metric*

$$d\ell^2 = g(u, v)(du^2 + dv^2),$$

then Gaussian curvature of the image of f, is

$$K = \frac{-1}{2g(u, v)} \Delta(\log g(u, v)) \tag{15}$$

where $\Delta = \frac{\partial^2}{\partial u^2} + \frac{\partial^2}{\partial v^2}$ is the Laplacian.

Proof. Let f and g be as described above. By Equation 5, we can express the curvature as

$$K = \frac{\begin{vmatrix} \frac{-1}{2}g_{vv} - \frac{1}{2}g_{uu} & \frac{1}{2}g_u & -\frac{1}{2}g_v \\ -\frac{1}{2}g_u & g & 0 \\ \frac{1}{2}g_v & 0 & g \end{vmatrix} - \begin{vmatrix} 0 & \frac{1}{2}g_v & \frac{1}{2}g_u \\ \frac{1}{2}g_v & g & 0 \\ \frac{1}{2}g_u & 0 & g \end{vmatrix}}{g^4}.$$

Expanding by cofactors and simplifying gives

$$K = \frac{-1}{2g}\left(\frac{gg_{vv} - g_v^2}{g^2} + \frac{gg_{uu} - g_u^2}{g^2}\right) \tag{16}$$

$$= \frac{-1}{2g}\left(\left(\frac{g_u}{g}\right)_u + \left(\frac{g_v}{g}\right)_v\right) \tag{17}$$

$$= \frac{-1}{2g}\left(\log(g)_{uu} + \log(g)_{vv}\right). \tag{18}$$

□

And now the proof of Theorem 6.7.

Proof. Let $p(z) = a_0 + a_1 z + \ldots + a_n z^n$ and, for the sake of contradiction, assume that $p(z) \neq 0$ for all $z \in \mathbb{C}$ and $a_0 a_n \neq 0$. We can define two new functions using $p(z)$. Set $p_*(z) = a_n + a_{n-1}z + \ldots + a_0 z^n$ and note that $p_*(z) = z^n p(1/z)$ for $z \in \mathbb{C} \setminus \{0\}$. Then let $f(z) = p(z)p_*(z)$ for all $z \in \mathbb{C}$. Then f has the property that

$$\left|f\left(\frac{1}{z}\right)\right| = \frac{1}{|z|^{2n}}|f(z)|,$$

for $z \in \mathbb{C} \setminus \{0\}$. The above property gives a well-defined metric g on $\widehat{\mathbb{C}}$ where

$$g = \frac{1}{|f(z)|^{\frac{2}{n}}}|dz|^2, \text{ for } z \in \mathbb{C} \text{ and}$$

$$g = \frac{1}{|f(1/z)|^{\frac{2}{n}}}|d(1/z)|^2 \text{ for } z \in \widehat{\mathbb{C}} \setminus \{0\}.$$

Now, for every $z \in \widehat{\mathbb{C}}$ we have

$$\frac{1}{|f(z)|^{\frac{2}{n}}}K = \frac{1}{n}\Delta(\log|f(z)|) = \frac{1}{n}\Delta\mathbf{Re}\log(f(z)) = 0. \tag{19}$$

The first equality in Equation 19 is by Theorem 6.10, the second equality is by our complex logarithm fact, Lemma 6.9, and the third equality is because the real part of an analytic function is harmonic, Lemma 6.8. Thus, the Gaussian curvature at every point is zero. However, the Gauss-Bonnet theorem states that the sum of the curvature over all $z \in \mathbb{C}$ is 4π, meaning there is at least one point where the curvature must be positive. This is a contradiction. □

References

[1] P. Alliez, D. Cohen-Steiner, O. Devillers, B. Lévy, and M. Desbrun. Anisotropic polygonal remeshing. *ACM Trans. Graph.*, 22(3):485–493, 2003.

[2] P. Alliez, M. Meyer, and M. Desbrun. Interactive geometry remeshing. *ACM Trans. on Graph.*, 21(3):347–354, 2002.

[3] J. M. Almira and A. Romero. Yet another application of the Gauss-Bonnet Theorem for the sphere. *Bulletin of the Belgian Mathematical Society - Simon Stevin*, 14(2), June 2007.

[4] M. F. Atiyah and I. M. Singer. The index of elliptic operators on compact manifolds. *Bulletin of the American Mathematical Society*, 69(3):422–433, 1963.

[5] T. F. Banchoff. Critical Points and Curvature for Embedded Polyhedral Surfaces. *The American Mathematical Monthly*, 77(5):475, May 1970.

[6] S. M. Bersten and H. B. Short. Small cancellation theory and automatic groups. *Invent. Math.*, 102:305–334, 1990.

[7] C. Blatter. Another Proof of Pick's Area Theorem. *Mathematics Magazine*, 70(3):200–200, June 1997.

[8] O. Bonnet. Mémoire sur la théorie générale des surfaces. *Journal de l'École Polytechnique*, 19(32):1–146, 1848.

[9] A. C. Bovik, editor. *Handbook of image and video processing.* Academic Press series in communications, networking and multimedia. Academic Press, San Diego, 2000.

[10] M. Carlsson. The gauss-bonnet theorem and applications to pseudospheres. *Uppsala University Project Report*, 41:1–24, 2021.

[11] B. Chazell and L. Palios. Triangulating a nonconvex polytope. *Disc. & Comp. Geom.*, 5(5):505–526, 1990.

[12] B. Chazelle. Convex partitions of polyhedra: A lower bound and worst-case optimal algorithm. *SIAM Jour. on Comp.*, 13:488–507, 1984.

[13] B. Chazelle and N. Shouraboura. Bounds on the size of tetrahedralizations. *10th ACM Symp. on Comput. Geom.*, pages 205–219, 1994.

[14] L. Chen and Y. Rong. Digital topological method for computing genus and the Betti numbers. *Topology and its Applications*, 157(12):1931–1936, Aug. 2010.

[15] S.-S. Chern. A Simple Intrinsic Proof of the Gauss-Bonnet Formula for Closed Riemannian Manifolds. *Annals of Mathematics*, 45(4):747–752, 1944.

[16] A. Christian. Course notes. *https://www.math.ucla.edu/ archristian/teaching/120a-f18/week-6.pdf*, 2018.

[17] P. Deigard. Liouville's equation on simply connected domains. Degree Project in Mathematics Uppsala University, 2020.

[18] M. P. do Carmo. *Differential geometry of curves and surfaces.* Prentice Hall, 1976.

[19] P. Dombrowski. *150 years after Gauss' disquisitiones generales circa superficies curvas*. Number 62 in Astérisque. Société mathématique de France, 1979.

[20] B. A. Dubrovin, A. T. Fomenko, and S. P. Novikov. *Modern Geometry — Methods and Applications*, volume 93 of *Graduate Texts in Mathematics*. Springer, New York, NY, 1984.

[21] D. Eppstein. Twenty-one proofs of euler's formula. Retrieved 25 June 2022. https://www.ics.uci.edu/ eppstein/junkyard/euler/.

[22] J. Erickson. Homotopy testing on surfaces. Retrieved 5 August 2022. Video Lecture 21.

[23] J. Erickson and K. Whittlesey. Transforming curves on surfaces redux. *24th ACM Symp, on Disc. Algo.*, pages 1646–1655, 2013.

[24] S. Fushida-Hardy. Two results in discrete geometry. Retrieved 7 August 2022.

[25] C. F. Gauss. *Disquisitiones generales circa superficies curvas*. Göttingen, 1827. Commentationes Societatis Regiae Scientiarum Gottingensis, Vol. 6.

[26] G. W. Gibbons and M. C. Werner. Applications of the Gauss-Bonnet theorem to gravitational lensing. *Classical and Quantum Gravity*, 25(23):235009, Dec. 2008.

[27] D. H. Gottlieb. All the Way with Gauss-Bonnet and the Sociology of Mathematics. *The American Mathematical Monthly*, 103(6):457, June 1996.

[28] P. Grinfeld. *Introduction to Tensor Analysis and the Calculus of Moving Surfaces*. Springer, New York, NY, 2013.

[29] V. Guillemin and A. Pollack. *Differential topology*. AMS Chelsea Pub, Providence, R.I, 2010.

[30] P. S. Heckbert and M. Garland. Optimal triangulations and quadric-based surface simplification. pages 49–65, 1999.

[31] D. Hilbert and S. Cohn-Vossen. *Geometry and the Imagination.* AMS Chelsea Publishing ; v.87. American Mathematical Society, Providence, 2021.

[32] T. Kaczynski, K. Mischaikow, and M. Mrozek. Computing homology. *Homology, Homotopy and Applications*, 5(2):233–256, 2003.

[33] T. Kong and A. Rosenfeld. Digital topology: Introduction and survey. *Computer Vision, Graphics, and Image Processing*, 48(3):357–393, Dec. 1989.

[34] M. Levi. A "bicycle wheel" proof of the gauss-bonnet theorem. *Expositiones Mathematicae*, 12:145–164, 1994.

[35] J. Liouville. *Sur la Theorie de la Variation des constantes arbitraires*, volume 3. Journal de mathématiques pures et appliquées, 1838.

[36] J. Matoušek. *Using the borsuk-ulam theorem*. Universitext. Springer, 2008.

[37] M. Meyer, M. Desbrun, P. Schröder, and A. H. Barr. Discrete differential-geometry operators for triangulated 2-manifolds. In *Visualization and Mathematics III. Mathematics and Visualization*, pages 35–57. Springer Berlin Heidelberg, 2003.

[38] J. R. Munkres. *Topology*. Pearson, second edition, 2000.

[39] J. O'Rourke. *Computational geometry in C*. Cambridge University Press, Cambridge ; New York, 1994.

[40] G. Pick. Geometrisches zur zahlentheorie. *Sitzenber. Lotos (Prague)*, 19:311–319, 1899.

[41] G. Polya. An Elementary Analogue to the Gauss-Bonnet Theorem. *The American Mathematical Monthly*, 61(9):601, Nov. 1954.

[42] A. Pressley. *Elementary Differential Geometry*. Springer Undergraduate Mathematics Series. Springer London, London, 2010.

[43] G. Rotskoff. The gauss-bonnet theorem. *University of Chicago Mathematics REU*, 2010.

[44] S. Tabachnikov. Proofs (Not) from The Book. *The Mathematical Intelligencer*, 36(2):9–14, June 2014.

[45] W. P. Thurston. *The Geometry and Topology of Three-Dimensional Manifolds*, volume 1. Princeton University Press, 1997.

[46] F. Tirado. Gauss-bonnet, s'il vous plaît. *Nebraska Conference for Undergraduate Women in Mathematics*, 2010. Undergraduate Thesis.

[47] S. Upadhyay. Gauss-bonnet for discrete surfaces. *University of Chicago Mathematics REU*, 2015.

[48] H.-H. Wu. Historical development of the Gauss-Bonnet theorem. *Science in China Series A: Mathematics*, 51(4):777–784, Apr. 2008.

[49] K.-L. Wu, T.-J. Ho, S. A. Huang, K.-H. Lin, Y.-C. Lin, and J.-S. Liu. Path Planning and Replanning for Mobile Robot Navigation on 3D Terrain: An Approach Based on Geodesic. *Mathematical Problems in Engineering*, 2016:1–12, 2016.

[50] D. G. Zill and P. D. Shanahan. *A First Course in Complex Analysis with Applications*. Jones & Bartlett Learning, 2nd edition, 2008.